Prediction errors bidirectionally bias time perception

Prediction errors bidirectionally bias time perception

Ido Toren, Kristoffer C. Aberg, Rony Paz

Department of Neurobiology, Weizmann Institute of Science, Rehovot, Israel

Abstract

Time perception and prediction errors are essential for everyday life. We hypothesized that their putative shared circuitry in the striatum might enable these two functions to interact. We show that positive and negative prediction errors bias time perception by increasing and decreasing perceived time, respectively. Imaging and behavioral modelling identifies this interaction to occur in the putamen. Depending on context, this interaction may have beneficial or adverse effects.

Correspondence should be addressed to: R.P (rony.paz@weizmann.ac.il)

Time perception in the sub-second range is essential for many animal behaviors[1]. Subjective perception is affected by motivational and emotional states, which usually increase perceived duration[2,3]. Learning is driven by efficient processing of reinforcement signals, and mainly by prediction error(PE)[4,5]: outcomes can be better than expected, a positive prediction error (PE+), or worse than expected, a negative prediction error (PE-). Although classically independent processes, recent studies suggest time perception and PE might be related[6,7]. Time perception engages striatal regions and their dopaminergic inputs[8,9], and neural correlates of PEs have been found in the same circuits. Moreover, PE+/PE- have been associated with increased/decreased activation of dopaminergic neurons, respectively[4,10], and perceived duration could be increased/decreased by activation/deactivation of dopaminergic neurons[11]. In addition, time perception is compromised in Parkinson disease and other basal-ganglia/dopamine related disorders[12,13]. We therefore hypothesized that signed prediction errors would differentially affect the perceived duration of a stimulus, and that such bias would be associated with differential striatal activity.

Participants determined which of two sequentially presented images is of longer duration in a 2-alternative-forced-choice paradigm (2AFC, Fig.1a). There were two types of trials: 'Short-Long' (SL) where the duration of the first image was shorter, and 'Long-Short' (LS). The difference in time duration between the two images (Δt) varied across trials. Each image was overlaid by a number indicating a monetary gain or loss.

Assuming a reference-dependent model of value where subjects learn to predict the relative outcome[14,15], the value of the first image serves as a reference point for predicting the value of the second image. Therefore, a prediction error would be PE+ if the difference between the images' values is larger than expected, and PE- if the difference is smaller than expected. A PE0 occurs when the difference was as expected. Importantly, a trial's outcome was determined only by the numbers presented on the images and was completely independent of the time discrimination performance (correct/incorrect). A first study established the behavioral bias, and a consecutive fMRI study replicated the behavior and elucidated the neural correlates (n=18/35).

An opposite bias of PE+ and PE- on perceived duration

Because discrimination is easier for larger values of Δt, we indeed found a significant main effect of Δt (Fig.1b; no significant interaction between PE-type and Δt, or three-way interaction). In line with our hypothesis, we found a significant interaction between PE type and Trial type (SL/LS) (Fig.1c). This result was robust for each group separately (behavior-only and fMRI), and also when considering the different PE magnitudes (Extended Data Fig.1,2,3).

What drives this interaction between PE type and Trial type? In our design, the PE occurs only when the second stimulus appears. Therefore, in SL trials when the value induces a PE+/PE-, if the image is perceived as longer/shorter, it would lead to a perceived larger/smaller Δt between the two stimuli resulting in easier/harder discrimination and hence better/worse performance. For LS trials, PE+/PE- would induce the opposite change in perceived Δt resulting in an opposite effect on performance.

Accordingly, we observed better performance in SL trials for PE+ compared to PE- and to PE0, and trials with PE- showed worse performance compared to PE0. The opposite pattern occurred in LS trials: performance was worse in PE+ compared to PE- trials and to PE0 trials, and PE- showed better performance compared to PE0 (Fig.1c).

Together, the results demonstrate that PE+ and PE- induce an increase and decrease in the perceived stimulus duration, respectively.

The contribution of order, individual thresholds, value and expectation

A second consecutive stimulus may bias the perceived duration of the first stimulus, termed Time-Order Error (TOE). Here, this would induce more errors in SL trials because the first image would be perceived as longer (Fig.1c; Extended Data Fig.4a,5). To account for this, we quantified the individual TOE and normalized performance accordingly (Fig.1c-Inset; Fig.1d; Extended data Fig.5). As expected, the main effect of Trial type was no longer significant, nor was the interaction between Trial type and Δt, whereas all other results, and importantly the significant interaction between PE type and Trial type, remained significant (Fig.1c-inset, Fig.1d).

We further accounted for individual differences by normalizing the objective Δt by each subject's just-noticeable-difference (JND). All findings were replicated using the individually-normalized psychometric curves (Fig.1e, Extended data Fig.1e,2e,3e). There was no overall change in perceptual thresholds (Extended Data Fig.6b), indicating that the bias is due to the instantaneous PE imposed in a trial.

We performed several control experiments to confirm that the bias is due to PE, rather than to valence or the outcome of the second image. First, we found that if the difference between the 1st and the 2nd image is predictable (even if it holds value), time perception is not altered (Extended Data Fig.6b; Supp. Information). Second, the results were replicated in a similar experiment but when all values were positive, i.e. where PE+/PE- include only gains. Finally, the results were replicated when the value in the second image was fixed, and PE+, PE0, or PE- were respectively induced by different values on the first image (Extended Data Fig.7*)*. Therefore, time perception is biased by the processing of signed PEs, and not by the valence (gains/losses) or the magnitude.

Modelling the PE-time bias and brain activations

To provide a trial-by-trial and individual information, we adapted a reinforcement-learning (RL)-based approach that considers main factors affecting the perceived duration: the objective time difference (Δt), the bias due to PE (θ), and the TOE (ε). According to the main findings, PE- decreases the perceived duration of the second image, which decreases/increases the perceived difference in SL/LS trials, respectively; and an opposite bias occurs in PE+ trials (Fig.1f). The Expected Value (EV) is the expected difference between the value in the second and the first images throughout the experiment, and is updated on a trial-by-trial basis (Extended Data Fig.4b). The probability of making a correct discrimination is then modeled by a logistic function and fitted individually for each subject. This model successfully captured individual behavior (Fig.2a,b; Extended Data Fig.2f, 3f), performance (Fig.2c), and TOE (Fig.2d). The bias magnitude (θ) was similar across PE+ and PE- (Fig.2e). To further validate the model accuracy, notice it estimates a continuous PE value, and we therefore replicated the main result (PE-type*Trial-type interaction) with several different thresholds ($|PE0|<0.005/0.01/0.1/0.2/0.5$).

Using the model-derived trial-by-trial PEs as parametric modulators, we identified brain regions previously shown to be involved in PE encoding: the ventral striatum, midbrain, and dorsal ACC (Fig.2f, Extended Data Fig.8, Supplementary Table 1).

In addition, we used the estimated probability for a discrimination-error as reflecting fluctuations of uncertainty in the perceptual task, and found a negative correlation (higher activation with low error-probability) in Brodmann 47 (Fig.2g-right) and between the nucleus accumbens and ventral ACC (Fig.2f-left), previously implicated in perceptual confidence (Supplementary Table 2). These findings strengthen the model validity and show that it integrates prediction error and time estimations in our task to capture variability in perceptual judgements.

Putamen activity corresponds to the PE-time bias

Because both time perception and prediction error involve striatal activity, we hypothesized that interaction in the striatum could contribute to the PE-time bias. We therefore conducted a whole-brain analysis using two-way ANOVA with factors PE type and performance (incorrect/correct), designed to identify regions that underlie the effect of PE leading to differences in performance, namely the PE time perception bias.

We found a significant interaction between PE type and performance in the putamen (Fig.3a). During PE+ trials, activation in the putamen was increased for incorrect compared to correct discriminations, whereas during PE- trials the putamen was de-activated for incorrect compared to correct judgements. This was the case both when including PE0 trials and when omitting them. Moreover, the individual difference in putamen activity between PE+ and PE- was correlated across correct and incorrect trials (Fig.3b). A significant interaction was also found in the dorsal ACC (Fig.3c, Supplementary Tables 3,4) with individual relationship when considering separately PE+ vs. PE0 and PE0 vs. PE- (Fig.3d).

Finally, to further establish a link between regional activations and the behavioral PE-time bias, we quantified the interaction in putamen activity and correlated it with the behavioral bias at an individual level (Fig.3e,f: lower-insets). These results suggest a direct link between interaction of activity in the putamen for PE and time duration, and the behavioral bias that PE induces on time perception.

Conclusions

Our findings provide evidence that prediction errors bias time perception, and suggest that interaction between these two fundamental functions is driven by interaction in striatal activations. We found a bidirectional effect, where a positive prediction error results in over-estimation of duration, and negative prediction error results in under-estimation of duration. These findings calls for revisiting the notion that arousal alone, during either negative[16] or positive stimuli[17], dictates longer perceived duration, and that predictability may induce shorter perceived duration[18]. The bidirectional bias that accompanies signed prediction error cannot be accounted for by absolute (attention-like) signals. A more integrative mechanism that combines differential patterns of attention due to valence, saliency[19], information[20], and unpredictability[18], might account for our findings.

Because both these processes are essential for daily tasks, the impact of such biases on learning and memory formation that rely on computations of predictions errors on one hand and on estimating durations on the other, can be of major importance. Therefore, the overlap in striatal activity that underlies the behavioral bias can either be an evolutionary benefit or an unfortunate by-product, for example, by influencing temporal-difference learning[6,7]. Abnormal interactions in striatal circuits underlying time duration and PE driven learning can therefore underlie and contribute to psychopathologies.

Acknowledgments: We thank Dr. Edna Furman-Haran and Fanny Attar for MRI procedures. This work was supported by a Joy-Ventures grant, ISF #2352/19 and ERC-2016-CoG #724910 grants to R. Paz.

Author contribution

I. T. and R. P. designed the study. I. T. performed the experiments and analyzed the data. K.C.A. contributed ideas for analysis. I. T., K.C.A. and R. P. wrote the manuscript.

Declaration of interests

The authors declare no competing interests.

References

1. Mauk, M.D. & Buonomano, D.V. The neural basis of temporal processing. *Annu. Rev. Neurosci.* **27**, 307-340 (2004).
2. Dirnberger, G., *et al.* Give it time: Neural evidence for distorted time perception and enhanced memory encoding in emotional situations. *NeuroImage* **63**, 591-599 (2012).
3. Droit-Volet, S. & Meck, W.H. How emotions colour our perception of time. *Trends Cogn Sci* **11**, 504-513 (2007).
4. Schultz, W., Dayan, P. & Montague, P.R. A neural substrate of prediction and reward. *Science* **275**, 1593-1599 (1997).
5. Niv, Y. & Schoenbaum, G. Dialogues on prediction errors. *Trends Cogn Sci* **12**, 265-272 (2008).
6. Petter, E.A., Gershman, S.J. & Meck, W.H. Integrating Models of Interval Timing and Reinforcement Learning. *Trends Cogn Sci* **22**, 911-922 (2018).
7. Mikhael, J.G. & Gershman, S.J. Adapting the flow of time with dopamine. *J Neurophysiol* **121**, 1748-1760 (2019).
8. Coull, J. & Nobre, A. Dissociating explicit timing from temporal expectation with fMRI. *Current opinion in neurobiology* **18**, 137-144 (2008).
9. Jahanshahi, M., Jones, C.R., Dirnberger, G. & Frith, C.D. The substantia nigra pars compacta and temporal processing. *J Neurosci* **26**, 12266-12273 (2006).
10. D'ardenne, K., McClure, S.M., Nystrom, L.E. & Cohen, J.D. BOLD responses reflecting dopaminergic signals in the human ventral tegmental area. *Science* **319**, 1264-1267 (2008).
11. Soares, S., Atallah, B.V. & Paton, J.J. Midbrain dopamine neurons control judgment of time. *Science* **354**, 1273-1277 (2016).
12. Allman, M.J. & Meck, W.H. Pathophysiological distortions in time perception and timed performance. *Brain* **135**, 656-677 (2012).
13. Jones, C.R. & Jahanshahi, M. Motor and perceptual timing in Parkinson's disease. *Advances in experimental medicine and biology* **829**, 265-290 (2014).
14. Bavard, S., Lebreton, M., Khamassi, M., Coricelli, G. & Palminteri, S. Reference-point centering and range-adaptation enhance human reinforcement learning at the cost of irrational preferences. *Nature communications* **9**, 1-12 (2018).
15. Klein, T.A., Ullsperger, M. & Jocham, G. Learning relative values in the striatum induces violations of normative decision making. *Nature communications* **8**, 16033 (2017).
16. Fayolle, S., Gil, S. & Droit-Volet, S. Fear and time: Fear speeds up the internal clock. *Behavioural processes* **120**, 135-140 (2015).
17. Smith, S.D., McIver, T.A., Di Nella, M.S. & Crease, M.L. The effects of valence and arousal on the emotional modulation of time perception: evidence for multiple stages of processing. *Emotion* **11**, 1305 (2011).
18. Eagleman, D.M. Human time perception and its illusions. *Current opinion in neurobiology* **18**, 131-136 (2008).
19. Failing, M. & Theeuwes, J. Reward alters the perception of time. *Cognition* **148**, 19-26 (2016).
20. Tse, P.U., Nobre, A. & Coull, J. Attention underlies subjective temporal expansion. *Attention and time*, 137-150 (2010).

Figure legends

Figure 1. Prediction errors bidirectionally bias time perception.

a. The 2AFC time-discrimination task. Example of Short-Long (SL) trial with PE0 (left) or with PE+ / PE- (right).

b. Proportion of discrimination errors as a function of objective time difference between the two images (Δt), averaged across all trials separately for each PE-type. Shown is the main effect of Δt (3-way ANOVA, $F_{4,208} = 98.7$, $p < 10^{-46}, \eta^2 = 0.65$).
Upper two insets show two individual subjects (all trials). Lower inset shows the proportion of discrimination errors in the first and second half of the experiment, indicating no change in perception throughout the experiment.

c. Proportion of discrimination errors as a function of PE type and Trial type. An interaction between PE type and Trial type ($F_{2,104} = 19.04$, $p < 10^{-7}, \eta^2 = 0.268$). SL trials: mean PE+ = 0.32, mean PE- = 0.49, mean PE0 = 0.43. Better performance in PE+ vs. PE- ($p < 10^{-5}, \text{Cohen's d} = 0.79$) and PE0 ($p = 0.0001, \text{Cohen's d} = 0.61$), worse performance in PE- compared to PE0 ($p = 0.02, \text{Cohen's d} = 0.36$). LS trials: mean PE+ = 0.33, mean PE- = 0.22, mean PE0 = 0.275. Worse performance in PE+ vs. PE- ($p = 0.0004, \text{Cohen's d} = 0.56$), and better performance in PE- compared to PE0 ($p = 0.02, \text{Cohen's d} = 0.39$).
Main effect of Trial type due to Time-Order Error (TOE) ($F_{1,52} = 26.19$, $p < 10^{-5}$, $\eta^2 = 0.33$). Inset: after correction for individual TOE, no main effect for Trial type, whereas the main interaction remains (PE type x Trial type: $F_{2,104} = 19.04$, $p < 10^{-7}, \eta^2 = 0.268$).

d. Proportion of discrimination errors as a function of (Δt), separately for LS and SL trials and corrected for TOE. PE+ and PE- bias performance in opposite directions relative to PE0, for all values of Δt.

e. Proportion of discrimination errors as a function of subjective Just-Noticeable-Difference (JND), corrected for TOE, fitted to a logistic function after JND normalization, and replicating the main finding (PE type * Trial-type, $F_{2,96} = 17.26$, $p < 10^{-6}, \eta^2 = 0.264$).

f. Schematic representation of the PE-time bias and the model. Right and left sides of the scheme represent LS and SL trials, respectively. Rectangles represent perceived duration of the images, with colors indicating different factors affecting the perceived duration: Gray represent the objective reference duration (t); Yellow denotes the time difference Δt added to the first or second image; Blue represent the change in the first image due to the TOE; and Pink represent the bias due to PE (θ), added or subtracted for PE+ or PE- (the main finding). Last row shows the prediction for the perceived duration, denoted by a dashed rectangle.
Inset shows real data, same as (c).

Error bars and error bands represent SEM (n=53).

Figure 2. Modelling the PE-time bias

a. Model fit to individual behavioral data, averaged over all subjects (n=53). Data points represent mean ±SEM, lines represent average over model fits ± SEM.
b. Two subjects' (rows) behavior and model fit. Left: model-derived probability of error, with blue/red circles indicating actual correct/incorrect discrimination, respectively. Right: actual outcome overlaid on model-derived expected value.
c. Difference between model-derived PE values is correlated between correct and incorrect trials, validating individual model-derived values (Pearson, r = 0.95, $p < 10^{-28}$).
d. The correlation between model-estimated TOE and that computed directly from behavior (Pearson, behavior-only group: r = 0.73, $p < 10^{-3}$; fMRI group: r = 0.83, $p < 10^{-5}$).
e. The correlation between the bias computed separately for PE+ and for PE- trials (Pearson correlation; behavior-only group: r = 0.73, $p < 10^{-3}$; fMRI group: r = 0.83, $p < 10^{-5}$). The bias magnitude was also similar (two-samples t-test; t_{51} = -1.1, p = 0.26). We therefore used a single bias in the model.
f. Brain ROIs where activation correlates with trial-by-trial model-derived PE+ signals (n=35). Time courses represent mean % signal change extracted from the ROIs ± SEM. Black vertical lines represent trial onset, offset and average onset of next trial, respectively. Activation was set to statistical threshold of q = 0.055 for visualization.
g. Activations in ventrolateral PFC/OFC (right) and NAc/vACC (left) correlate with model-derived probability for correct discrimination (n=35). Average activation ± SEM for correct and incorrect choices is plotted below, showing higher activation for correct discriminations. Inset shows the mean probability for discrimination error.

Figure 3. Putamen activity underlies PE-time interaction and behavioral bias

a. Activation in the anterior right putamen is associated with an interaction between PE-type (PE+, PE-) and time discrimination accuracy (correct or incorrect responses). Mean parameter estimates (beta) for PE-type and performance extracted from ROI. Also shown are the corresponding time-course activations. Inset shows individual data points. Error bars represent SEM (n=35).
b. Individual-subject putamen activations (extracted from the above ROI) for PE+/PE- in incorrect vs. correct discrimination trials, showing an interaction between PE type and performance at an individual level (Pearson; $r = 0.45$, $p = 0.005$).
c. Same as (a) for the dorsal anterior cingulate cortex (dACC; n=35). Inset shows individual data points.
d. Individual subject dACC activations (extracted from the above ROI) for PE+/PE0 (left) and PE0/PE- (right) in incorrect vs. correct discrimination, showing an interaction between PE-type and performance at an individual level (Pearson; PE+/PE0: $r = 0.37$, $p=0.03$; PE-/PE0: $r = 0.6$, $p<0.0001$).
e. Individual interaction score for putamen activity is correlated with the individual behavioral bias (θ). Shown is the distribution of p-values using bootstrap (two-sided test, 20% with $p<0.05$, dashed red line and red bars, significantly different than expected, $p<0.001$, Fisher's test). Upper inset show the significantly right-skewed distribution of the correlation coefficients. Lower inset shows the correlation for the original data.
f. Same as in (d) when the model includes a separate bias for PE+ and for PE- ($\theta+$ and $\theta-$), revealing an even closer match between behavioral bias and activation patterns in the Putamen (42% with $p<0.05$, $p<0.001$, Fisher's test).

Methods

Experimental design

Participants

Eighteen (18) healthy participants (5 males) participated in the behavior-only group and 35 healthy right-handed participants (15 males) participated in the imaging group (fMRI). Additionally, 19 participants (8 males) participated in a gain-only control group. Subjects' age varied between 22-40. In the imaging group, mean age was 26 and median age was 25. No statistical methods were used to pre-determine sample sizes but our sample sizes are similar to those reported in previous publications. All studies were approved by the Helsinki committee of the Sourasky medical center, protocol number 0287-09-TLV (Ministry of health protocol #HT5271), and further approved by the IRB of the Weizmann Institute. All participants had normal or corrected-to normal vision and reported no attention deficit hyperactivity disorder (ADHD). Informed consent was obtained from all participants prior to the experiment. Participants were compensated for their time, and according to the accumulation of gains and losses in the experiment (but no less than the minimum payment as determined in the protocol). Compensation was independent of the performance in the time discrimination task. All investigators were blind to any group, subject or sequence allocation during data collection and analyses. One participant in the imaging group was unable to complete the fMRI scan due to unexpected stress inside the magnetic field and another participant could not complete the scan due to extensive movements, and both had been excluded.

Visual stimuli

White images with black numbers displayed in the center of the image were presented on a gray background. The images were identical in size, presented in the center of a 21" screen with refresh rate of 60 Hz (lag smaller than 1ms), and spanning a visual angle of approximately 5.1º x 3.8º, with a red fixation cross displayed before the image appears. In all tests stimulus presentation was implemented by MATLAB (R2014b, MathWorks) using the Psychophysics Toolbox[21,22].

Time duration discrimination paradigm

Two images were presented sequentially with 0.5sec delay between them. After the presentation of the second image, participants had to determine which image had been presented for a longer duration (Fig.1a). One image was always displayed for a duration of 500 ms – the 'reference' duration, whereas the other image was presented for 500ms plus an additional duration (Δt). Because the Just Noticeable time Difference (JND) in time duration discrimination tasks have been reported to range around 15-20% of the standard duration[23,24], we set Δt in the present experiment to range from 0 ms (equal presentation time for both images) to 133 ms, corresponding to Δt of 0-26.6% of the 500 ms reference duration.

To generate prediction errors, numbers representing monetary gains and/or losses were overlaid on each image. The first image was always presented with the number zero, while the number of the second image could be negative - generating (PE-); zero - generating no PE (PE0), or positive - generating (PE+). To create a baseline expectation of the difference between values overlaid on the images (2^{nd} image – 1^{st} image), a large proportion of trials were PE0 trials (60% in the behavior-only group and 80% in the imaging group), with an

equally smaller proportion of trials being PE+ and PE- trials. For the behavior-only group, PEs were generated by presenting numbers ranging from -5 to +5, in steps of 0.5. For the imaging group, to avoid loss-aversion effects[25] in brain activity, we used twice the magnitude of PE+ compared to PE-[26], and PEs were generated by presenting either -2 (PE-), 0 (PE0), or +4 (PE+). There was a uniform distribution of presentations across PE values (i.e. all values were presented in a similar number of trials; with the exception of PE0 trials). Moreover, the number of trials for each Δt was equal across PE values, with a counterbalanced and fully random order of presentation. Randomization of trials was used for all participants. For the imaging group, we used OPTSEQ2 software to determine sequence of trials and inter-trial-intervals prior to the experiment, and every subject was randomly assigned to a one of the generated sequences. The accumulation of monetary gains and losses corresponded to an actual monetary compensation provided at the end of the experiment. Importantly, the monetary compensation was independent of the performance on the duration discrimination task.

Gain only group

The paradigm for this group is largely similar to the main paradigm described above, with the following modifications: First, values on the images were positive only (+1,+2,+4), meaning that participants could only gain money in each trial. In addition, whereas for the other groups we fixed the value in the first image, here we allowed different values also in the first image. Specifically, in SL trials the first image was always overlaid with the number (+2), while the number of the second image could be either (+1) - generating (PE-); (+2) - generating no PE (PE0), or (+4) - generating (PE+). In LS trials, in contrast, the second image was always overlaid with the number (+2), while the number of the first image could be either (+1) - generating (PE+); (+2) - generating no PE (PE0), or (+4) - generating (PE-). Finally, as in the main group, 80% of the trials were PE0 trials, with an equally smaller proportion of trials being PE+ and PE- trials, and the Δt was varied in the same range and distribution, with one additional value of 83ms, corresponding to 16.6% of reference duration (500ms).

Just Noticeable Difference (JND) paradigm

JND estimates for each participant represent the minimal difference in time duration between two stimuli that can still be detected with high probability. Two psychophysical methods were used to estimate the JND in the present study. First, we used a one-up-two-down staircase procedure[27]. Specifically, in each trial two images were presented sequentially (one for 500 ms, the other for 500ms+Δt). If participants correctly discriminated which image was presented for the longer duration, the order of presentation was reversed, and if participants again made a correct discrimination, Δt was decreased by an adaptive amount of time. Whenever an incorrect discrimination was made, Δt was increased by the same amount (up to a maximum of 250 ms). Initial Δt was determined on 125 ms, with a 10% decrease of the step size after every trial (regardless of participants' discrimination accuracy). This process repeats itself until a stopping criterion of correct discrimination after cumulative 6 previous errors have been reached (number of trials was not limited), at which point a threshold has been determined which yields an expected value of 0.707 probability of making a correct discrimination. Of note, while numbers were presented on the images at all times, monetary gains and losses were only associated with the numbers at the test conducted at the end of the experiment (see *Procedure* below). The second procedure used the method-of-constant-stimuli (MCS) in which a fixed set of pre-determined Δt's (identical to main

paradigm) were used. Otherwise, the presentation of images was similar as before. The resulting data was then used to generate a psychometric curve for each participant, by fitting a generalized linear regression of the responses to a binomial distribution, and the threshold was defined as the Δt in which participants had a 0.707 probability of making a correct discrimination.

Constant-loss (no surprise) condition

Following the main task, all participants in the imaging group performed 40 additional trials using the same paradigm as in the main task, except that the second image value was always -2 while the first image value was always 0. This condition was designed to generate a 'constant loss' condition, where the trials are identical to PE- trials except of the predicted nature of outcomes. We therefore hypothesized that performance in 'constant loss' trials would resemble performance during main task PE0 trials, but would be different than performance during main task PE- trials, even though the images and outcomes are identical.

General procedure

Behavior-only group

Following general instructions, a JND time duration discrimination threshold was first estimated for each participant. JND estimate using the staircase procedure was conducted with a zero number overlaid on both images, and two additional JNDs were estimated using two MCS procedures of 40 trials each. In one of the MCS procedures, both the first and the second image had the number zero, while in the other MCS procedure the first image was presented with the number zero, while a random number was presented on the second image. This allowed us to control for threshold, visual confounds and value (Extended Data Fig.6a). Next, participants performed the time duration discrimination paradigm.

Imaging group

The procedure of the imaging group is largely similar to behavior-only group, with the following modification: JNDs were estimated outside the MRI scanner, before and after the main paradigm, and for all images and pairs. In the second estimation of JND (but not the first), after the scan, participants gained and lost money based on the numbers presented on the image, thus allowing us to control for reward value confounds. The time duration discrimination task and the 'constant loss' task was performed while undergoing fMRI scanning. Minimum of three training trials were provided inside the scanner to allow participants to become accustomed to the scanner.

Gain-only group

The procedure of the gain-only group was similar to the procedures described above: following instructions, a JND threshold was estimated using a staircase method followed by a time-duration discrimination paradigm. At the end of the experiment, the JND was re-evaluated.

TOE measures from behavior

A well-established perceptual phenomena is the Time Order Error (TOE), which predicts that the duration of the first stimulus in a sequence of stimuli with equal durations, is perceived as longer as compared to succeeding stimuli durations[28,29].

TOE can be defined as the difference in probability of successful discrimination as a function of Trial-type (i.e., Short-Long or Long-Short):

$$TOE = \frac{p(R_{10}|S_{10}) - p(R_{01}|S_{01})}{2} \quad [1]$$

Where R_{10} represent a response that the first stimulus is longer, and S_{10} represent LS trial, i.e. first stimulus is longer. R_{01}, S_{10} represent the opposite response (i.e. the second stimulus is longer) given a SL trial.

To compute the above we extracted individual performance during PE0 trials separately for every Δt, and used the resulted TOEs to correct the probability of discrimination error in all PE-type trials (Fig.1c-inset,1d, Extended Data Fig.1b-inset,1d, 2b-inset,2d, 3b-inset,3d):

$$corrected\_p(dt)_{SL} = observed\_p(dt)_{SL} - TOE(dt)$$
$$corrected\_p(dt)_{LS} = observed\_p(dt)_{LS} + TOE(dt) \quad [2]$$

Consequently, positive and negative TOE in time duration discrimination occurs if the first stimulus is perceived as having a longer and shorter duration, respectively. In our experiment, we found positive TOE across all Δt's (Extended Data Fig.4a), thus offering an explanation as to why the probability of making a mistake when Δt=0 (i.e. the duration of both images is identical) is different than chance level and opposite between LS and SL trials (Extended Data Fig.1c, 2c, 3c). Specifically, when the duration of the first image was longer (LS trials), TOE causes an even longer perceived duration, generating easier trials (larger perceived Δt). By contrast, when the duration of the first image is shorter (SL trials), TOE causes a shorter perceived duration, leading to more difficult trials (smaller perceived Δt).

To compute unbiased behavioral TOE (and compare it to the model-derived estimate), we took the intersection between performance in PE0 trials and 0.5 proportion of discrimination errors at Δt = 0.

Computational Modeling

Performance (the probability of making an incorrect discrimination) was modeled as a logistic function[24,30,31]:

$$p(\Delta t) = \frac{1}{1 + e^{-f(\Delta t)}} \quad [3]$$

We assume that performance depends linearly on Δt, i.e. larger Δt leads to better performance:

$$f(\Delta t) = b_1(\Delta t) + b_2 \quad [4]$$

Next, we address other parameters that could influence the perceived Δt.

First, we included the Time Order Error (TOE). We found positive TOE across all Δt's (Extended Data Fig.4a), which predicts that the duration of the first stimulus is perceived as of longer duration. TOE was here modeled by the parameter ε.

Second, the bias in time duration discrimination due to PE, here denoted by the parameter θ, is caused by the mismatch between the difference in outcomes presented in first and the

second image (2^{nd} –1^{st}), and the expected outcome difference. Namely, the value of the prediction error on trial *i* was computed as the difference between the actual presented values and current estimation of expected value (EV):

$$PE_i = (R_i - EV_{i-1}) \quad [5]$$

Where

$$R_i = R_{i,2^{nd}\ image} - R_{i,1^{st}\ image} \quad [6]$$

EV was initialized to 0 and was updated on every trial using a learning-rate parameter α:

$$EV_i = EV_{i-1} + \alpha * (R_i - EV_{i-1}) \quad [7]$$

Our results indicate that PE+ and PE- cause the duration of a stimulus to be perceived as longer and shorter, respectively. Accordingly, PE+ decreases performance in LS trials (causing the perceived duration of the second stimulus to be more similar to that of the first stimulus), and vice versa in SL trials. Incorporating ε and θ into the model gives the following expression:

$$f(dt) = b_1\left(\Delta t_i + k_1(\varepsilon + \theta * PE_i)\right) + b_2 \quad [8]$$

Where

$$k_1 = \begin{cases} -1, & SL\ trials \\ 1, & LS\ trials \end{cases}$$

Finally, one additional parameter γ was added to the model to account for a ceiling effect observed in LS trials (in these trials performance is initially much closer to the perceptual threshold (JND) due to TOE, thus might be bounded). The final model looks as follows:

$$f(dt) = (b_1 - \gamma) * \left(\Delta t_i + k_1(\varepsilon + \theta * PE_i)\right) + b_2 \quad [9]$$

Where

$$\gamma = \begin{cases} \gamma, & SL\ trials \\ 0, & LS\ trials \end{cases}$$

The model is then plugged into the logistic probability function and estimated separately for every subject.

Model parameters were estimated by computing the maximum a-posteriori (MAP) probability using MATLAB's function *fmincon* (MathWorks). We assumed uniform prior on the parameters and used bounds as follows:

$$b1 \in [-20,20]$$
$$b2 \in [-20,20]$$
$$\gamma \in [-10,10]$$
$$\theta \in [-2,2]$$
$$\varepsilon \in [-2,2]$$

$$\alpha \in [0,1]$$

To make sure that results are not biased due to outliers, we repeated the estimation process with a Gaussian distribution over each parameter with a mean 0 and variance X, where X equals to the bound described above for every parameter (e.g., θ was modeled as $N(0,2)$). Finally, we also computed unconstrained maximum likelihood of the parameters with no priors and no bounds (except from the learning rate which remained bounded) using MATLAB's function *fminunc*. All results are highly similar with respect to model fit and parameters values.

fMRI data acquisition

Images were acquired on a 3T Siemens MAGNETOM Tim-Trio scanner. Functional T2* weighted images were acquired using a gradient-echo EPI sequence (TR = 2000 ms, TE = 30 ms, flip angle = 75°, 32 slices with 10% gap scanned in a descending order with phase encoding direction anterior-to-posterior at 30° toward coronal from anterior commissure–posterior commissure (ACPC) plane[32], slice thickness 3 mm, voxel size 3x3x3 mm, FOV 216) in 5 separate scanning sessions (up to two minutes between sessions). Anatomical T1-weighted images were acquired after the functional scans (TR = 2300 ms, TE = 2.98 ms, flip angle = 9°, voxel size 1x1x1 mm, FOV 256). The anatomical scan covered the whole brain while functional scan covered the whole brain except a small area in the dorsal part of the parietal lobe. To improve signal-to noise ratio of the event-related design, order of trials and Inter-Trial-Interval (ITI) in the scanner was determined using OPTSEQ2[33].

All imaging data were preprocessed and analyzed using Brain Voyager QX 3.4 (Brain Innovation Maastricht, The Netherlands[34] and MATLAB R2014a (MathWorks) with BVQX/Neuroelf toolbox v1.0 (Jochen Weber, http://neuroelf.net/). Preprocessing included slice scan time correction, motion correction and high-pass filtering. Images were then co-registered and normalized into Talairach space[35] and spatially smoothed with an isotopic 6 mm FWHM Gaussian kernel.

Statistical analysis

Data analysis

Performance on the time duration discrimination task was estimated as the proportion of incorrect discriminations for each combination of PE-type (PE+, PE-, PE0), Trial-type (SL/LS), and Δt. These results were then analyzed via repeated measures ANOVAs with these factors and performance as the dependent variable. Post-hoc tests were done using Tukey-Kramer test, effect sizes were estimated by Cohen's d or η^2, and null results were estimated by Bayes Factor. Data distribution was assumed to be normal but this was not formally tested. Trials in which no response was made were discarded from analysis.

Normalization to JND

The objective Δt was normalized by each subject's staircase Just-Noticeable-Different (JND) measured at the beginning of the experiment. Normalization for every individual was done as follows: Δt values in ms were transformed to individual JND units, interpolated for a range of [0-1.5] JND and then fit to a logit function. Four (4) participants with no valid Just-Noticeable-Difference (JND) measure were pre-excluded from this analysis.

fMRI data analysis

Analyses consist of random effects Analysis of variance (ANOVA) based on general linear models (GLM), with event regressors defined from the onset of the first image until the offset of the second image, models as box-car functions and convolved with a canonical hemodynamic response function (HRF). All models included 6 regressors to account for head movements and a regressor to account for the motor response, modeled from the onset of the cue until the subject's response.

Multiple comparison correction on cluster size was done using non-parametric permutation test[36,37]. Null distribution of maximal cluster size was built separately using 1000 iterations for every analysis (PE x Correctness interaction, all trials with probability weights as parametric modulators). On every iteration, all labels of all trials were randomly shuffled for every subject, and a GLM for every voxel was computed using the same definitions as in main analysis. Finally, ANOVA model was created and maximum cluster size was extracted (direct or diagonal proximity in one dimension was sufficient to include voxels in same cluster) using the MATLAB function *bwlabeln*. Cluster Defining Threshold (CDT) level was set on $p < 0.005$.

Analysis using trial-to-trial PE estimates as parametric modulations consist of separate contrasts for PE-types and was corrected for multiple comparisons using false discovery rate of $q < 0.05$. Three (3) participants were pre-excluded from the trial-by-trial fMRI analysis because their modelled learning rate was zero, generating a regressor of zeros which cannot be included in this analysis.

Computational model selection

Our computational models were built to track trial-to-trial probability of discrimination error, corresponds to the behavioral measure used in analyses.

We tested 5 variations of the model:

Model 1 – The selected model (6 parameters; b_1, b_2, $\alpha, \varepsilon, \theta, \gamma$).

Model 2 – no free parameter b_2 (5 parameters).

Model 3 – no γ (5 parameters).

Model 4 – no b_2, no γ (4 parameters).

Model 5 – Separate parameters for the bias due to PE+ (θ^+) and PE (θ^-) (7 parameters).

For each model, AIC (Akaike Information Criterion) was estimated using the computed likelihood of the model for each subject regulated by the number of parameters. AICs were used as model evidence in a Bayesian Model Selection for group studies[38], in which the exceedance probabilities of all models (i.e., the probability that each model is more frequent in the population than other models) is estimated. Results indicated a 0.98 probability for model 1 to be the model best explaining the evidence, therefore it is the selected model.

Assigning PE-type to trials according to the computational model

In order to generate different trial types according to the modeled PE, trials were categorized based on the sign and the magnitude of the estimated PE. Since almost no trials estimated precisely PE=0, and in order to assign enough trials for all PE types to generate a valid statistic, we selected a threshold for which a trial with absolute value of PE smaller than that threshold would be assigned as a PE0 trial, and PE larger or smaller would be assigned as PE+ and PE- trials, respectively:

$$|\mathrm{PE}_i| < \text{threshold} : \text{trial i is PE0}$$
$$\mathrm{PE}_i \leq -\text{threshold} : \text{trial i is PE} -$$
$$\mathrm{PE}_i \geq \text{threshold} : \text{trial i is PE} +$$

A threshold of 0.1 was chosen since it produced a similar proportion of PE0 trials as in the actual design. To make sure that this selection did not bias the results, we also tested thresholds of 0.2, 0.5, 0.01, and 0.005. All tests resulted in the same main effects and interactions except the three-way interaction which wasn't significant for low (below 0.05) thresholds. This indicates a robust PE type statistic across different levels of classification.

Correlation between individual interaction activations and behavioral bias

We calculated an interaction-score for each subject's Putamen activity and correlated it with the individual behavioral bias (θ) derived from the model:

$$Interaction\_activity\_score = \big(\beta(PE+, Correct) - \beta(PE-, Correct)\big) - (\beta(PE+, InCorr) - \beta(PE-, InCorr)) \quad [10]$$

Where $\beta(PE+, Correct)$ is the average regional activity in trials of PE+ with correct response, and so forth. The Interaction_activity_score provides an approximate individual quantification of the interaction found in the imaging analysis (PE_TYPE * performance). To establish robustness of this measure we performed a bootstrap by resampling a different set of subjects every time and re-calculating the correlation between the Putamen interaction-factor and the behavioral bias for each subset of subjects. The distribution of the correlation coefficients and their respective p-values was estimated using Fisher's test.

Reporting Summary

Further information on research design is available in the Nature Research Reporting Summary linked to this article.

Code availability

Custom code for behavioral and imaging tests is available from the corresponding author upon reasonable request.

Data availability

All data supporting the findings of this study are available from the corresponding author upon reasonable request.

References

21. Brainard, D.H. & Vision, S. The psychophysics toolbox. *Spatial vision* **10**, 433-436 (1997).
22. Pelli, D.G. The VideoToolbox software for visual psychophysics: Transforming numbers into movies. *Spatial vision* **10**, 437-442 (1997).
23. Rammsayer, T. & Ulrich, R. The greater temporal acuity in the reminder task than in the 2AFC task is independent of standard duration and sensory modality. *Canadian Journal of Experimental Psychology/Revue canadienne de psychologie expérimentale* **66**, 26 (2012).
24. Ulrich, R. & Vorberg, D. Estimating the difference limen in 2AFC tasks: Pitfalls and improved estimators. *Attention, Perception, & Psychophysics* **71**, 1219-1227 (2009).
25. Kahneman, D. Prospect theory: An analysis of decisions under risk. *Econometrica* **47**, 278 (1979).
26. Tom, S.M., Fox, C.R., Trepel, C. & Poldrack, R.A. The neural basis of loss aversion in decision-making under risk. *Science* **315**, 515-518 (2007).
27. Levitt, H. Transformed up-down methods in psychoacoustics. *The Journal of the Acoustical society of America* **49**, 467-477 (1971).
28. Allan, L.G. The time-order error in judgments of duration. *Canadian Journal of Psychology/Revue canadienne de psychologie* **31**, 24 (1977).
29. Hellström, Å. The time-order error and its relatives: Mirrors of cognitive processes in comparing. *Psychological Bulletin* **97**, 35 (1985).
30. Laufer, O. & Paz, R. Monetary loss alters perceptual thresholds and compromises future decisions via amygdala and prefrontal networks. *Journal of Neuroscience* **32**, 6304-6311 (2012).
31. Taatgen, N.A., Van Rijn, H. & Anderson, J. An integrated theory of prospective time interval estimation: The role of cognition, attention, and learning. *Psychological Review* **114**, 577 (2007).
32. Deichmann, R., Gottfried, J.A., Hutton, C. & Turner, R. Optimized EPI for fMRI studies of the orbitofrontal cortex. *Neuroimage* **19**, 430-441 (2003).
33. Dale, A.M. Optimal experimental design for event-related fMRI. *Human brain mapping* **8**, 109-114 (1999).
34. Goebel, R., Esposito, F. & Formisano, E. Analysis of functional image analysis contest (FIAC) data with brainvoyager QX: From single-subject to cortically aligned group general linear model analysis and self-organizing group independent component analysis. *Human brain mapping* **27**, 392-401 (2006).
35. Talairach, J. & Tournoux, P. Co-planar stereotaxic atlas of the human brain. 3-Dimensional proportional system: an approach to cerebral imaging. (1988).
36. Eklund, A., Nichols, T.E. & Knutsson, H. Cluster failure: why fMRI inferences for spatial extent have inflated false-positive rates. *Proceedings of the National Academy of Sciences* **113**, 7900-7905 (2016).
37. Woo, C.-W., Krishnan, A. & Wager, T.D. Cluster-extent based thresholding in fMRI analyses: pitfalls and recommendations. *Neuroimage* **91**, 412-419 (2014).
38. Stephan, K.E., Penny, W.D., Daunizeau, J., Moran, R.J. & Friston, K.J. Bayesian model selection for group studies. *Neuroimage* **46**, 1004-1017 (2009).

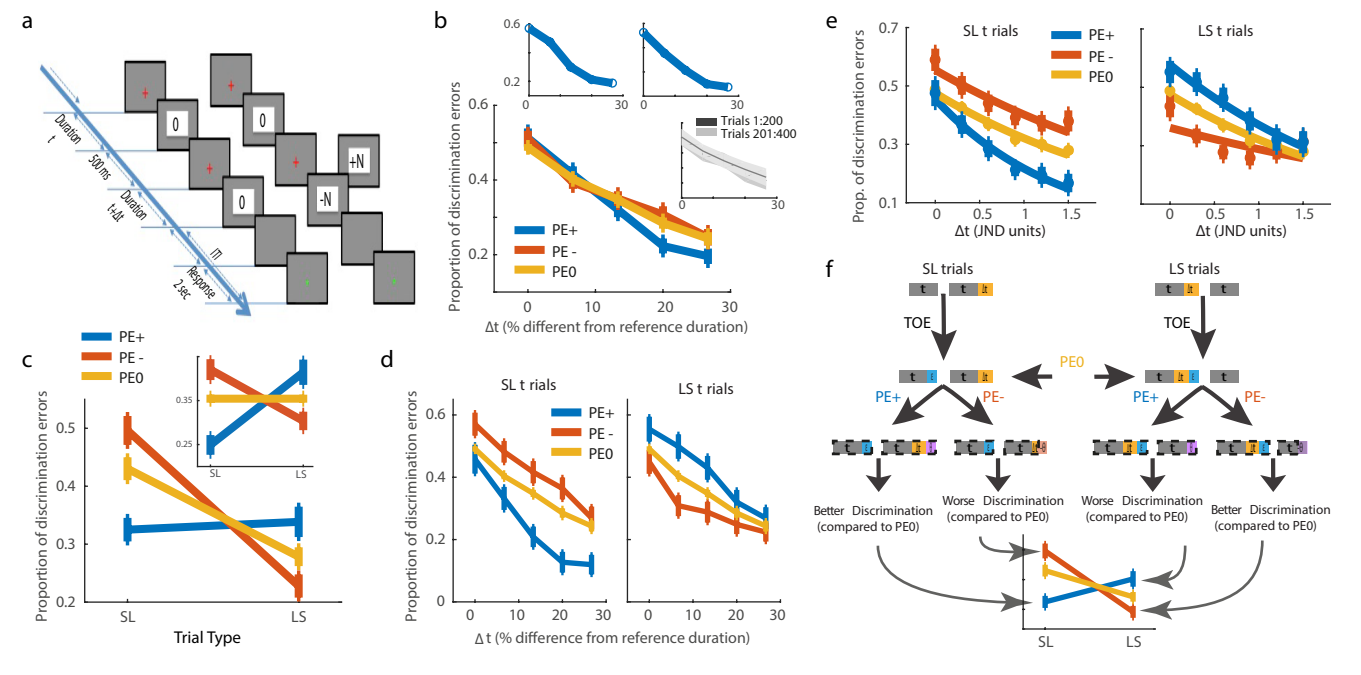
a
Duration
t
500 ms
Duration
t+Δt
ITI
Response
2 sec
0
0
0
+N
-N
b
Proportion of discrimination errors
Trials 1:200
Trials 201:400
PE+
PE -
PE0
Δt (% different from reference duration)
c
PE+
PE -
PE0
Proportion of discrimination errors
SL
LS
Trial Type
d
SL t rials
LS t rials
PE+
PE -
PE0
Proportion of discrimination errors
Δ t (% difference from reference duration)
e
SL t rials
LS t rials
PE+
PE -
PE0
Prop. of discrimination errors
Δt (JND units)
f
SL trials
LS trials
TOE
PE0
PE+
PE-
Better Discrimination (compared to PE0)
Worse Discrimination (compared to PE0)
Worse Discrimination (compared to PE0)
Better Discrimination (compared to PE0)
SL
LS

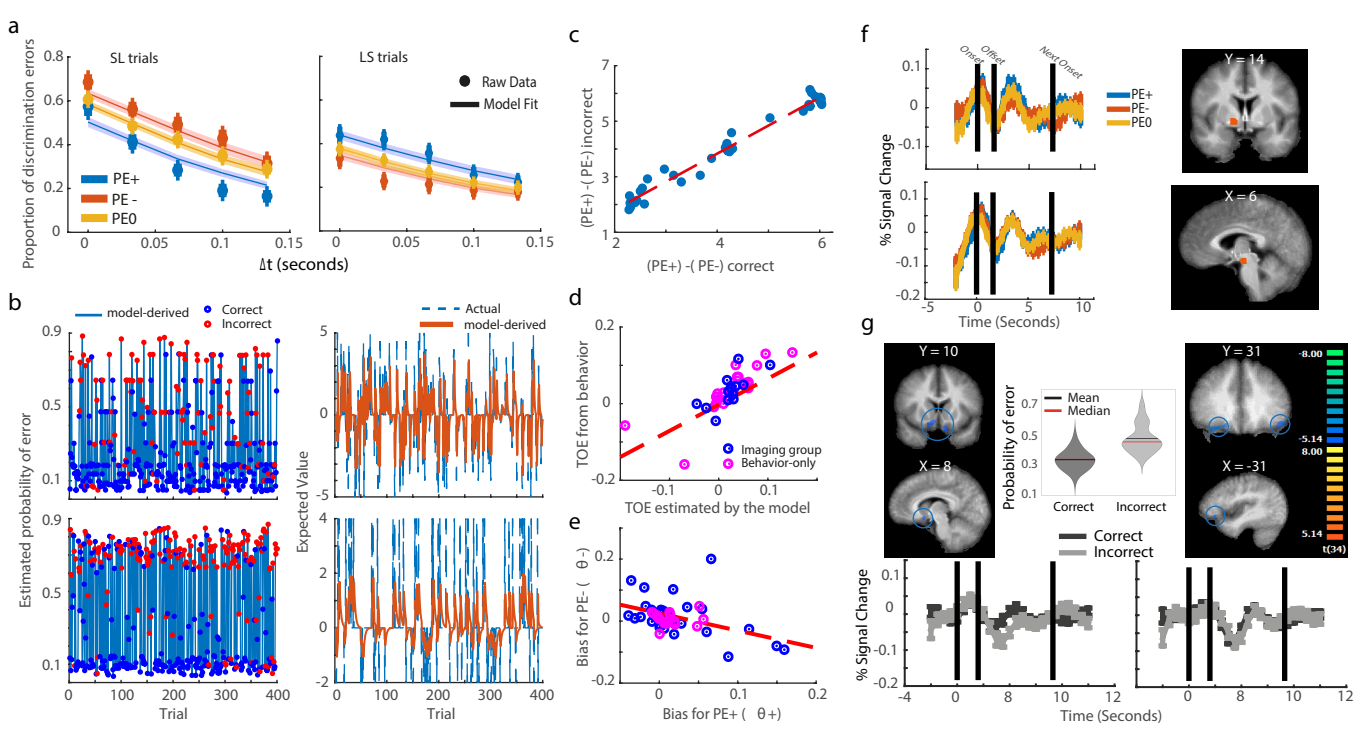
a
SL trials
LS trials
Raw Data
Model Fit
PE+
PE -
PE0
Proportion of discrimination errors
Δt (seconds)
b
model-derived
Correct
Incorrect
Actual
model-derived
Estimated probability of error
Expected Value
Trial
c
(PE+) -(PE-) incorrect
(PE+) -(PE-) correct
d
TOE from behavior
Imaging group
Behavior-only
TOE estimated by the model
e
Bias for PE- (θ -)
Bias for PE+ (θ +)
f
Onset
Offset
Next Onset
PE+
PE-
PE0
% Signal Change
Time (Seconds)
Y = 14
X = 6
g
Y = 10
X = 8
Mean
Median
Probability of error
Correct
Incorrect
Y = 31
X = -31
-8.00
-5.14
8.00
5.14
t(34)
Correct
Incorrect
% Signal Change
Time (Seconds)

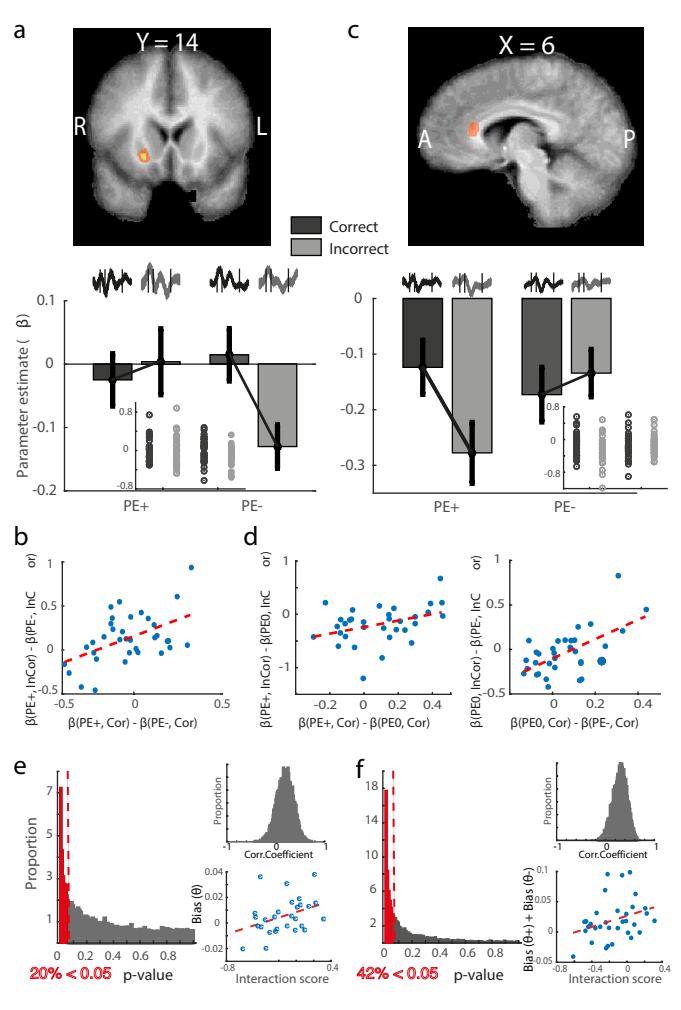
a
Y = 14
R
L
c
X = 6
A
P
Correct
Incorrect
Parameter estimate (β)
0.1
0
-0.1
-0.2
PE+
PE-
0
-0.1
-0.2
-0.3
0.8
0
-0.8
b
d
β(PE+, InCor) - β(PE-, InC
β(PE+, Cor) - β(PE-, Cor)
β(PE+, InCor) - β(PE0, InC
β(PE+, Cor) - β(PE0, Cor)
β(PE0, InCor) - β(PE-, InC
β(PE0, Cor) - β(PE-, Cor)
e
f
Proportion
Corr.Coefficient
Bias (θ)
Interaction score
20% < 0.05
p-value
42% < 0.05
Bias (θ+) + Bias (θ-)

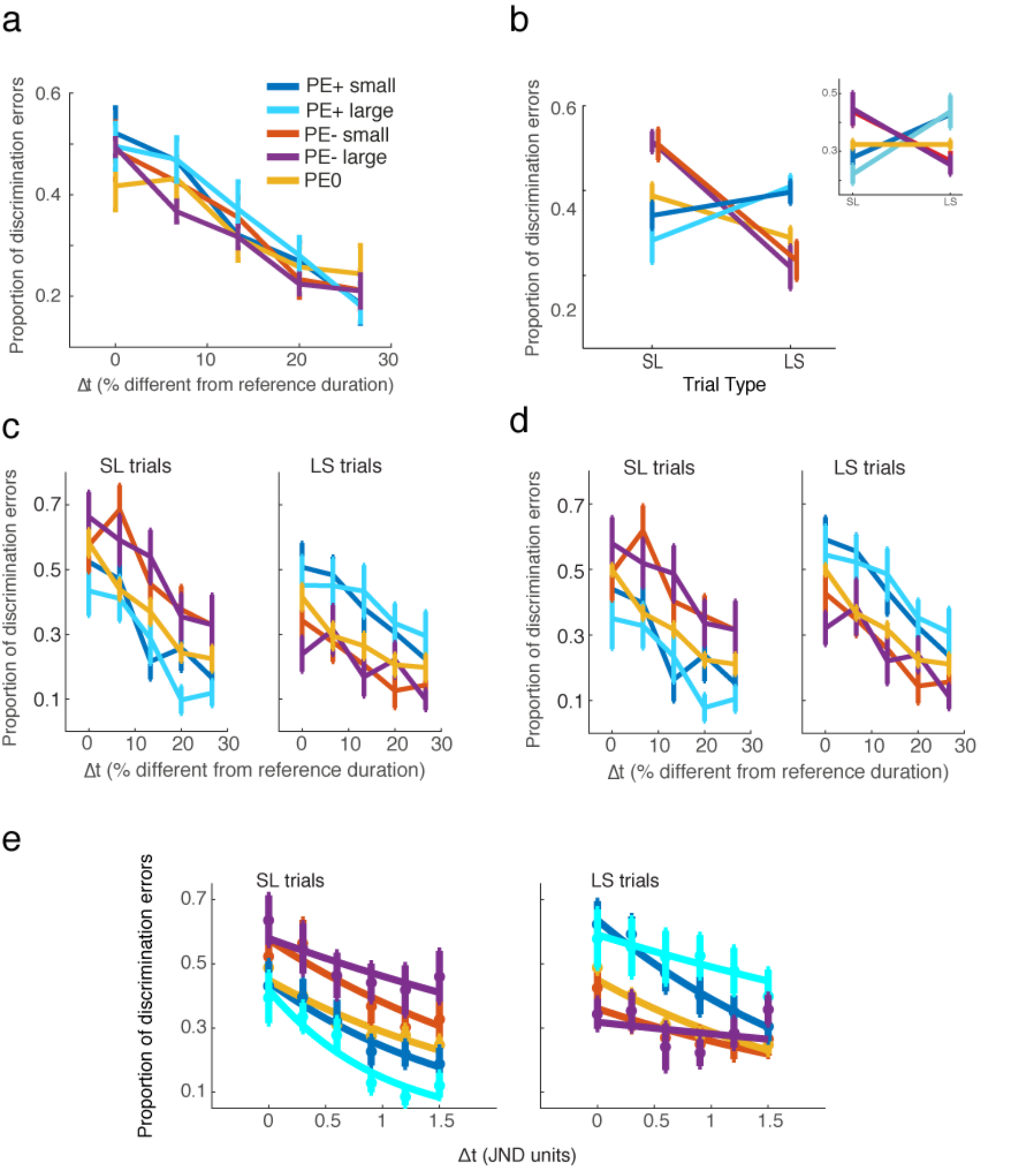
a
b
c
d
e
PE+ small
PE+ large
PE- small
PE- large
PE0
Proportion of discrimination errors
Δt (% different from reference duration)
Trial Type
SL
LS
SL trials
LS trials
Δt (JND units)

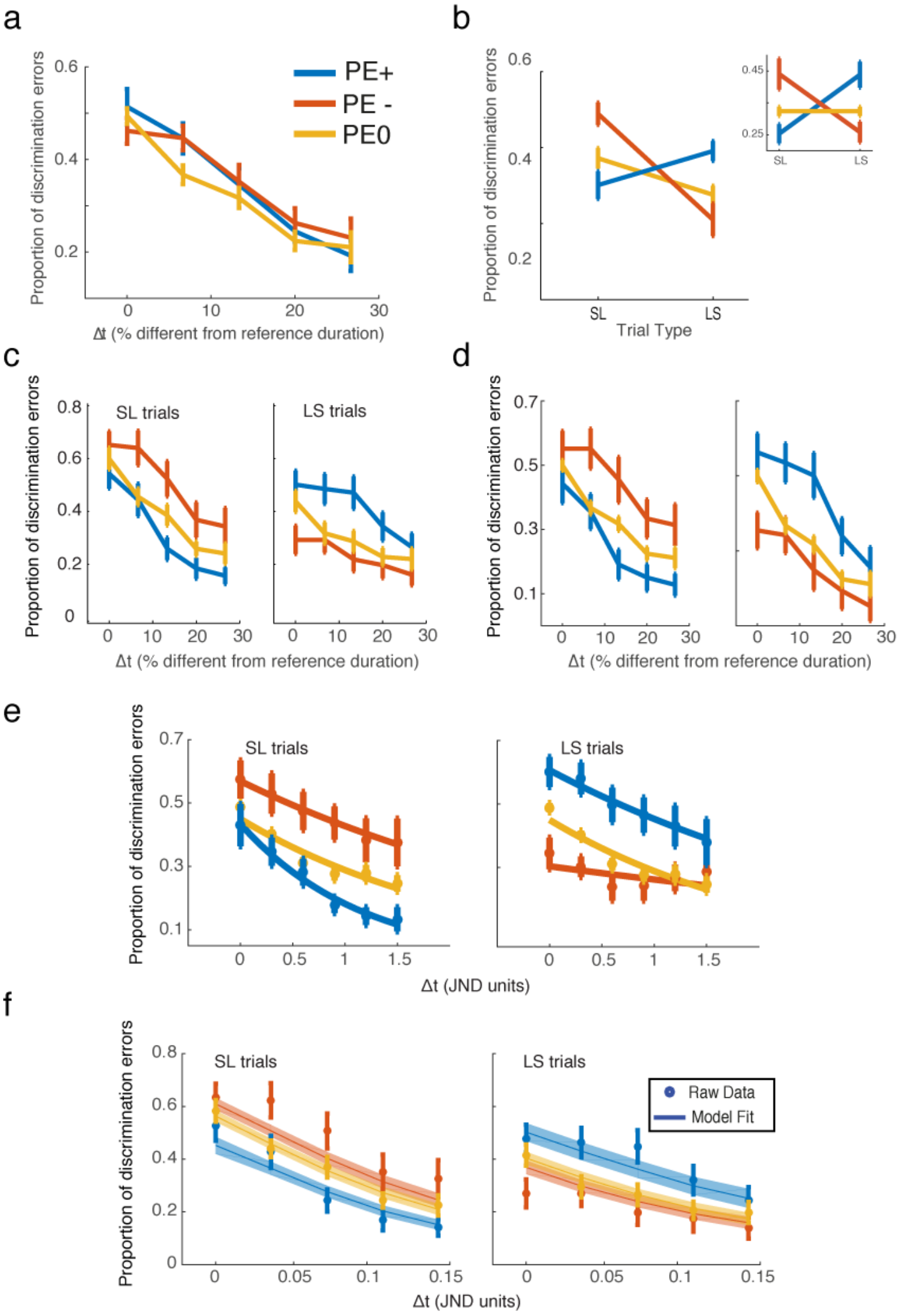
a
b
c
d
e
f
Proportion of discrimination errors
PE+
PE -
PE0
Δt (% different from reference duration)
Trial Type
SL
LS
SL trials
LS trials
Δt (JND units)
Raw Data
Model Fit

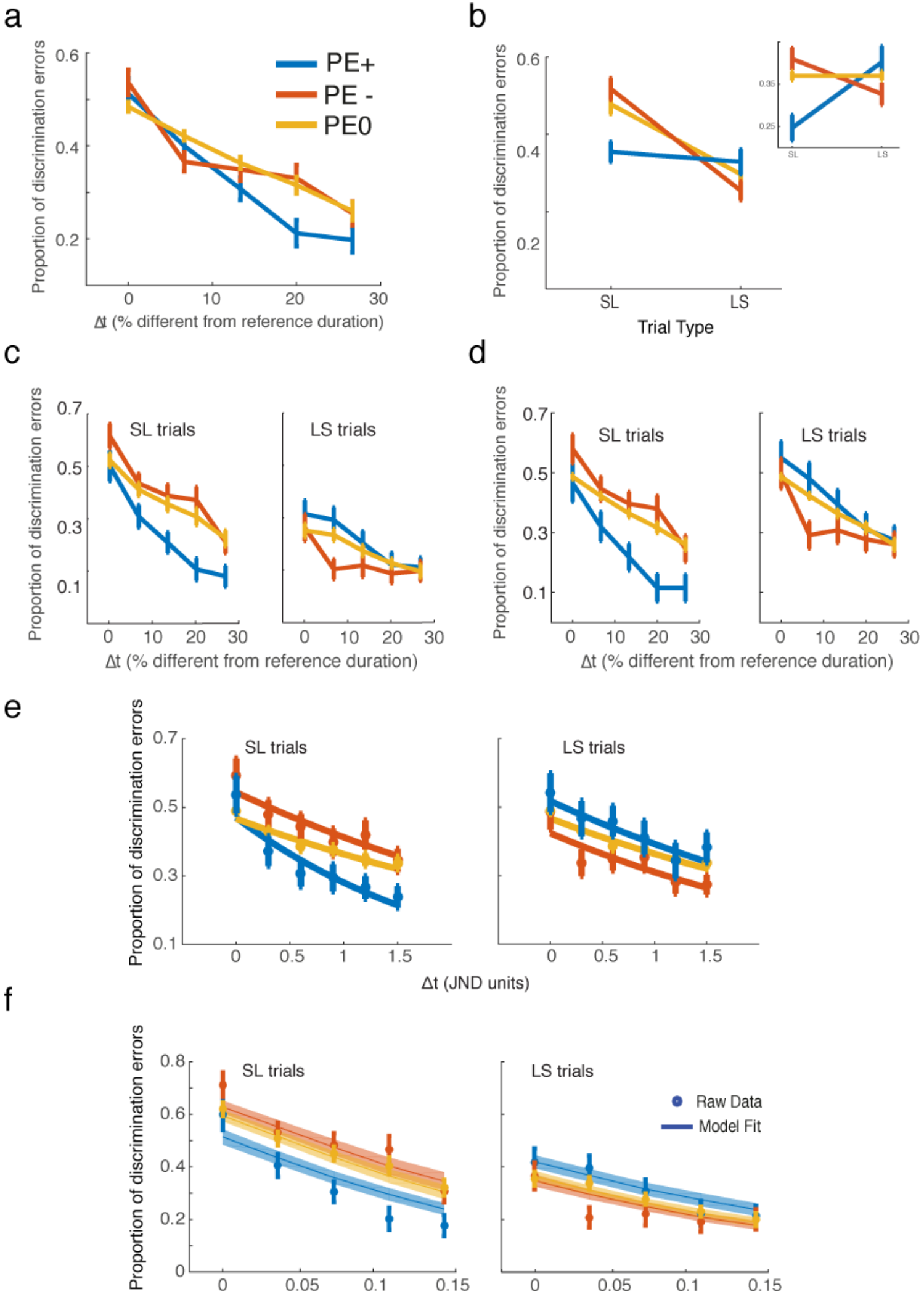
a
b
c
d
e
f
PE+
PE -
PE0
Proportion of discrimination errors
Δt (% different from reference duration)
Trial Type
SL
LS
SL trials
LS trials
Δt (JND units)
Raw Data
Model Fit

a

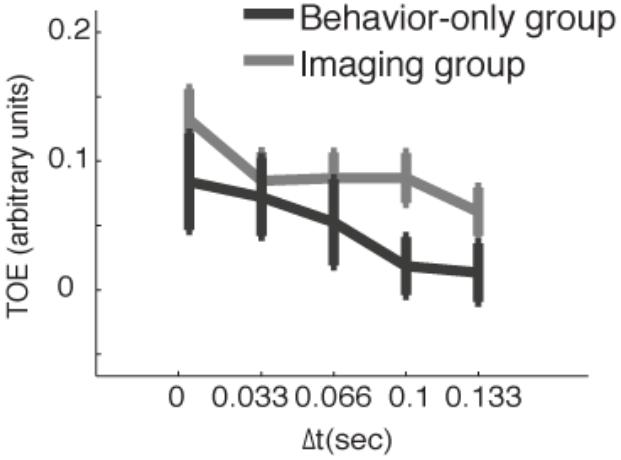
Behavior-only group
Imaging group
TOE (arbitrary units)
0.2
0.1
0
0
0.033
0.066
0.1
0.133
Δt(sec)

b

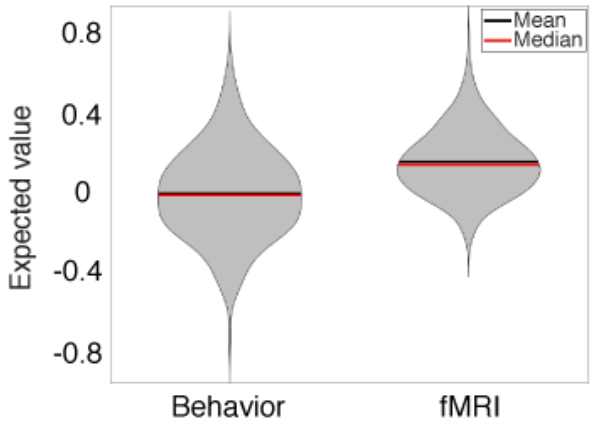
Mean
Median
Expected value
0.8
0.4
0
-0.4
-0.8
Behavior
fMRI

c

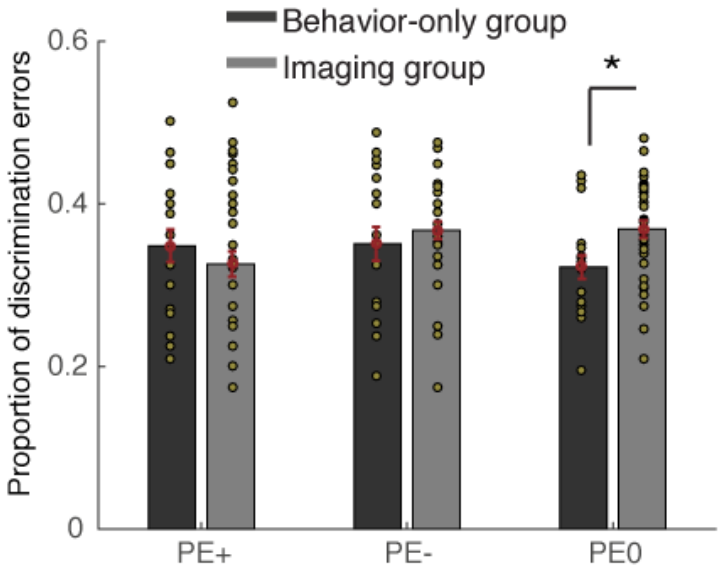
Behavior-only group
Imaging group
*
Proportion of discrimination errors
0.6
0.4
0.2
0
PE+
PE-
PE0

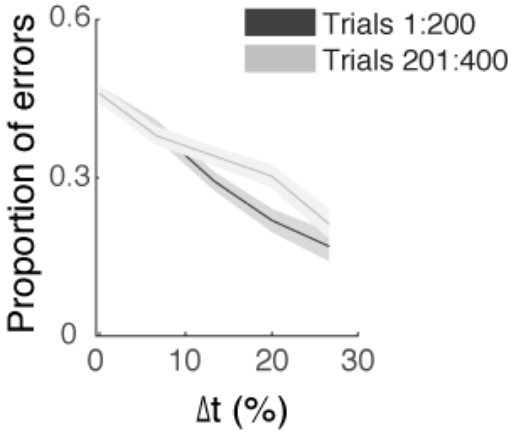
Trials 1:200
Trials 201:400
Proportion of errors
0.6
0.3
0
0
10
20
30
Δt (%)

a

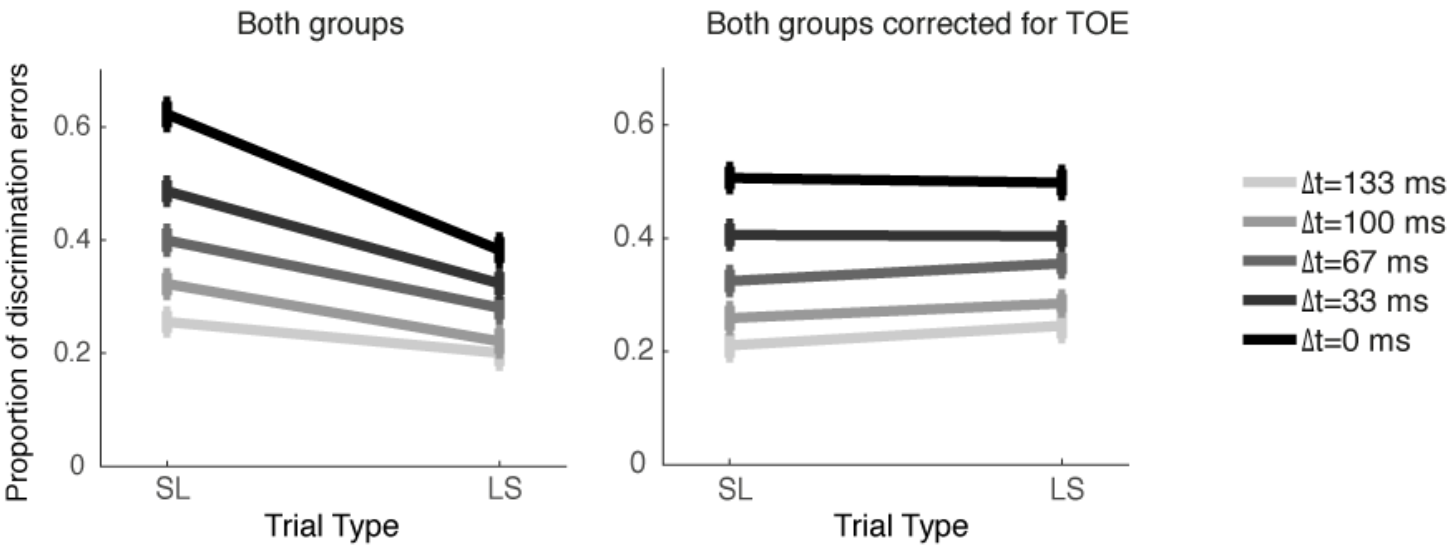
Both groups
Both groups corrected for TOE
Proportion of discrimination errors
0.6
0.4
0.2
0
SL
LS
Trial Type
Δt=133 ms
Δt=100 ms
Δt=67 ms
Δt=33 ms
Δt=0 ms

b

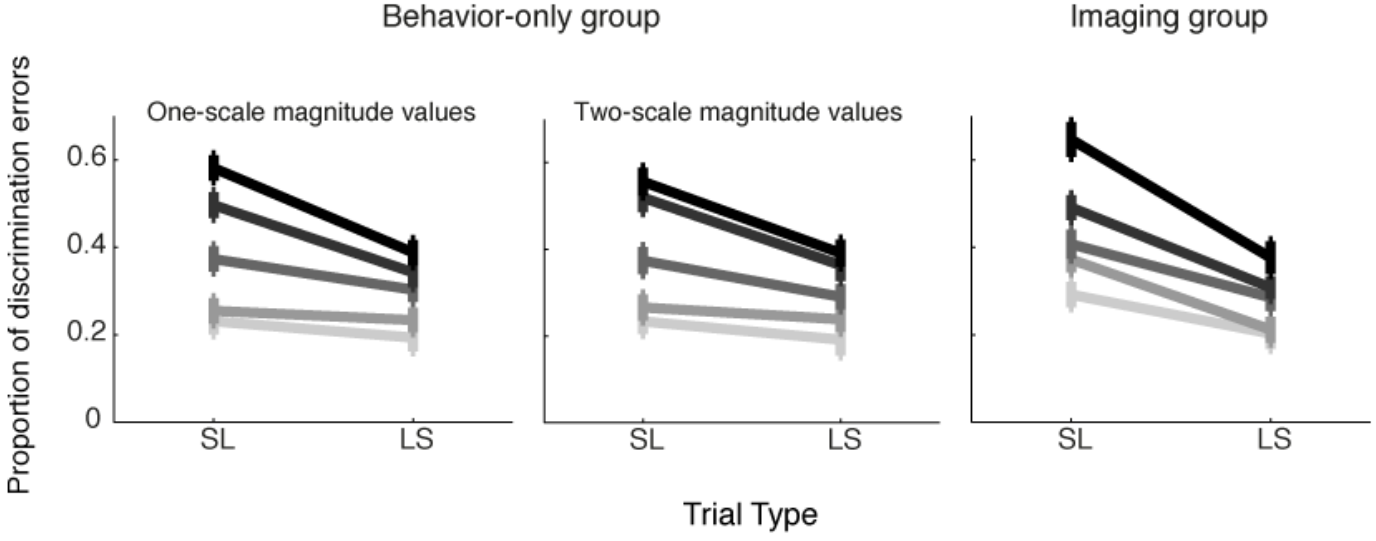
Behavior-only group
Imaging group
One-scale magnitude values
Two-scale magnitude values
Proportion of discrimination errors
0.6
0.4
0.2
0
SL
LS
Trial Type

a

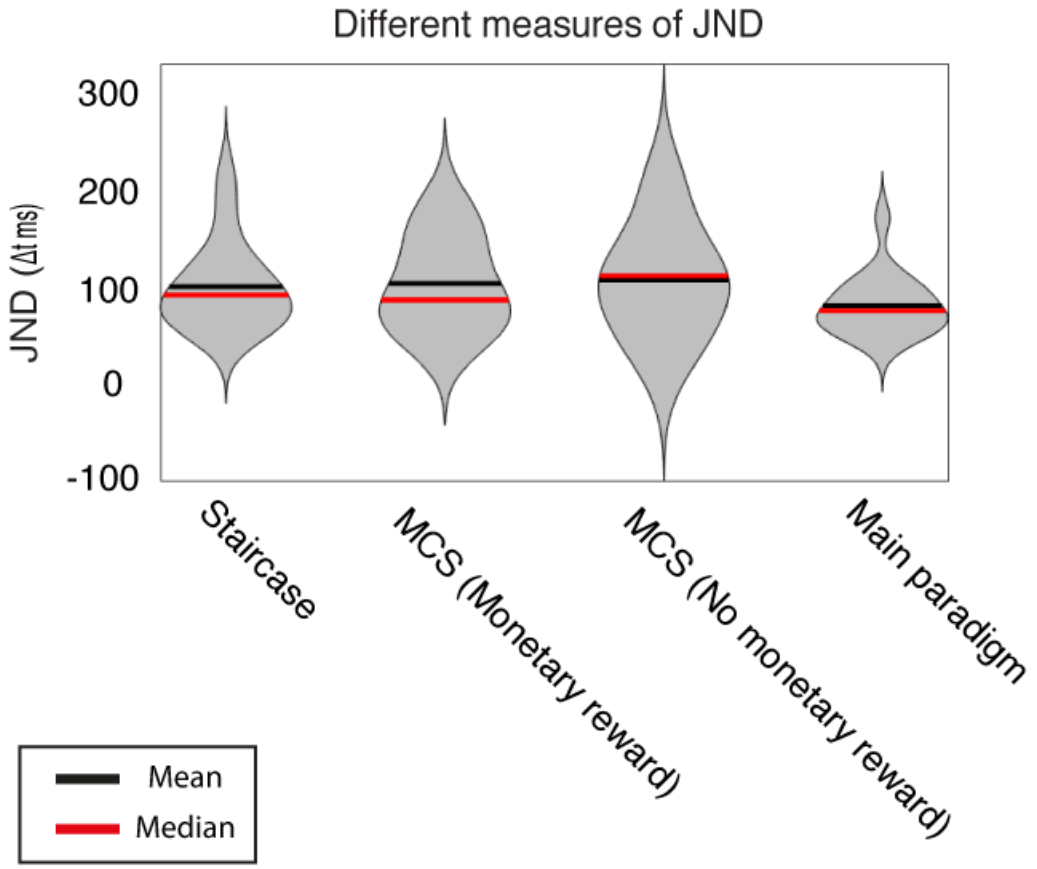
Different measures of JND
JND (Δt ms)
300
200
100
0
-100
Staircase
MCS (Monetary reward)
MCS (No monetary reward)
Main paradigm
Mean
Median

b

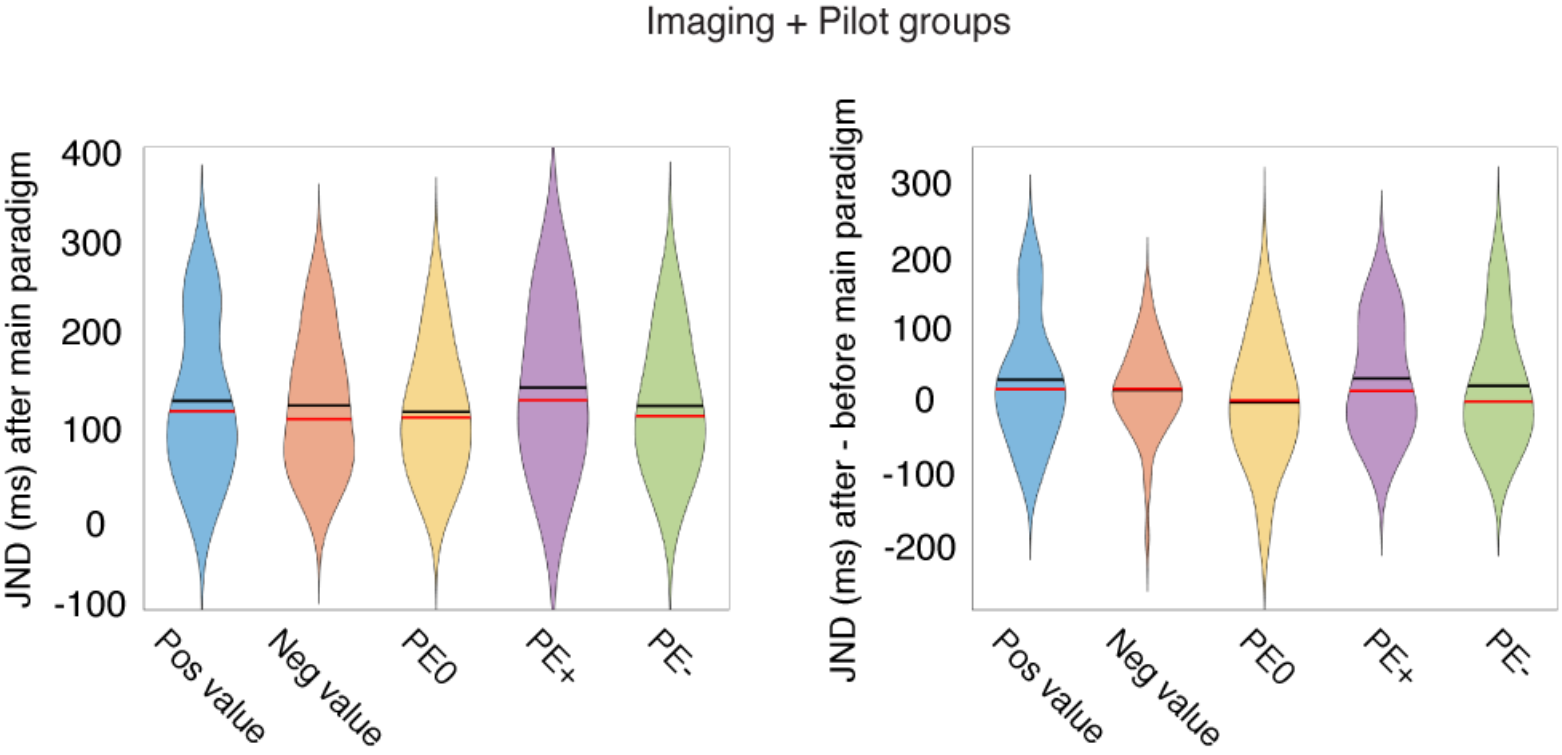
Imaging + Pilot groups
JND (ms) after main paradigm
400
300
200
100
0
-100
Pos value
Neg value
PE0
PE+
PE-
JND (ms) after - before main paradigm
300
200
100
0
-100
-200
Pos value
Neg value
PE0
PE+
PE-

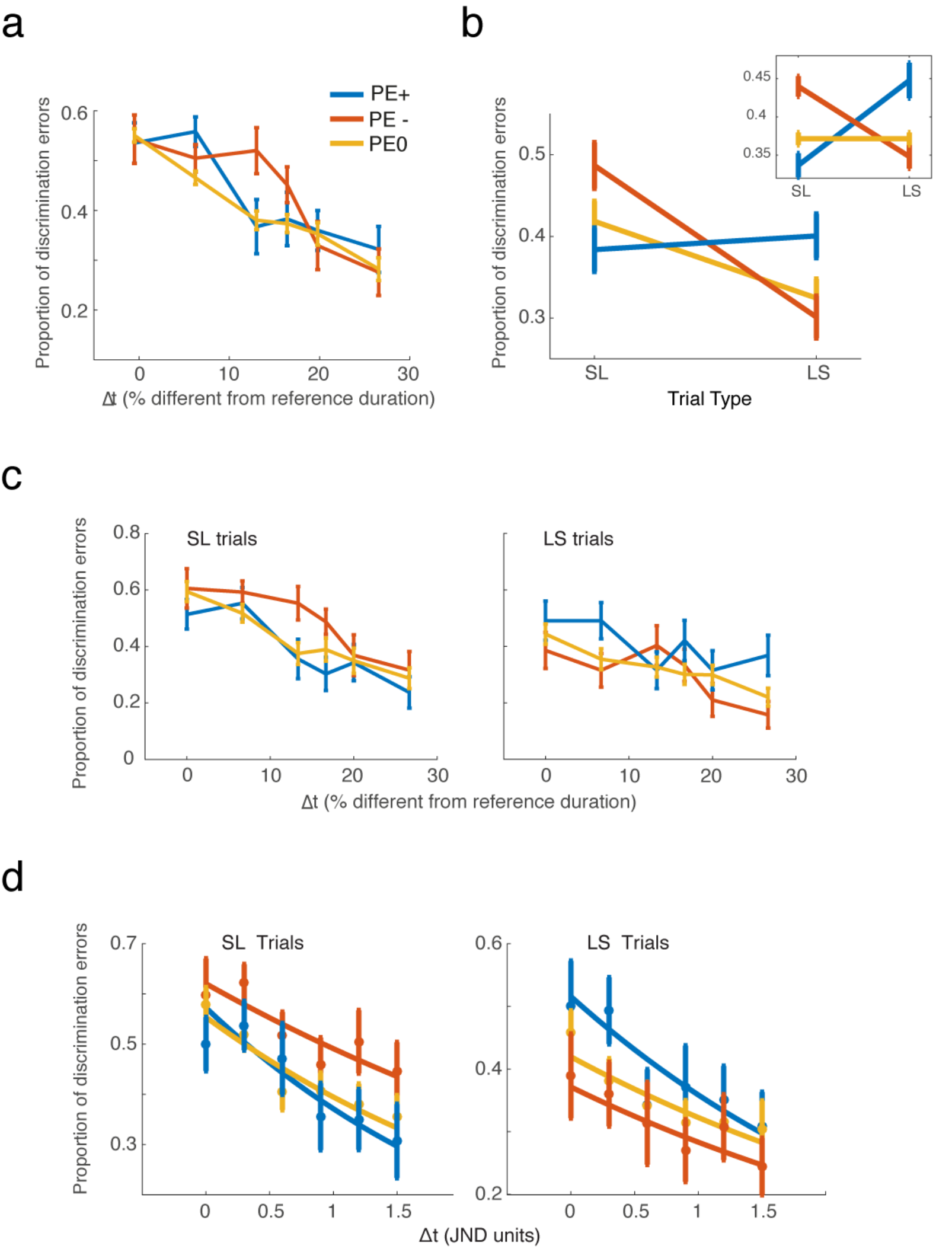
a
b
c
d
PE+
PE -
PE0
Proportion of discrimination errors
Δt (% different from reference duration)
Trial Type
SL
LS
SL trials
LS trials
SL Trials
LS Trials
Δt (JND units)

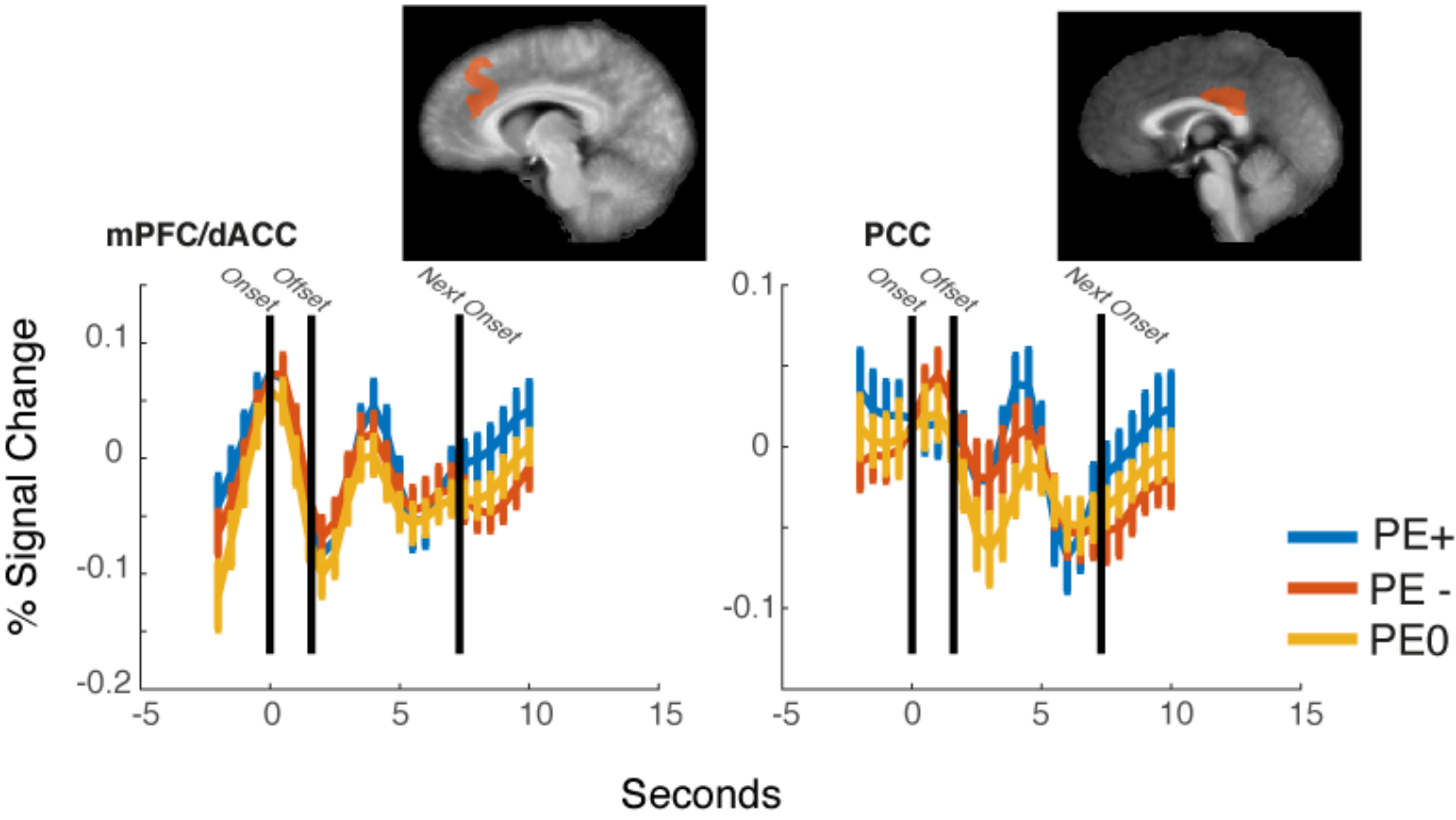
mPFC/dACC
PCC
Onset
Offset
Next Onset
0.1
0
-0.1
-0.2
-5
0
5
10
15
% Signal Change
Seconds
PE+
PE -
PE0